HHS Public Access

Author manuscript

Clin Cancer Res. Author manuscript; available in PMC 2020 July 01.

Published in final edited form as:

Clin Cancer Res. 2020 January 01; 26(1): 301–311. doi:10.1158/1078-0432.CCR-19-1063.

A PI3K/AKT Scaffolding Protein, IQ motif-containing GTPase Associating Protein 1 (IQGAP1), Promotes Head and Neck Carcinogenesis

Tao Wei[1], **Suyong Choi**[2], **Darya Buehler**[3], **Richard A. Anderson**[2], **Paul F. Lambert**[1,4]

[1]McArdle Laboratory for Cancer Research, University of Wisconsin School of Medicine and Public Health, Madison, Wisconsin.

[2]University of Wisconsin-Madison, School of Medicine and Public Health, Madison, Wisconsin.

[3]Department of Pathology and Laboratory Medicine, University of Wisconsin School of Medicine and Public Health, Madison, Wisconsin.

[4]Carbone Cancer Center, University of Wisconsin School of Medicine and Public Health, Madison, Wisconsin.

Abstract

Purpose—Head and neck cancer (HNC) is the sixth most common cancer worldwide with a 5-year survival rate of less than 50%. The PI3K/AKT/mTOR signaling pathway is frequently implicated in HNC. Recently, IQ motif-containing GTPase activating protein 1 (IQGAP1) was discovered to scaffold the PI3K/AKT signaling pathway. *IQGAP1* gene expression is increased in HNC, raising the hypothesis that IQGAP1 contributes to HNC.

Experimental Design—We performed a combination of *in vitro* studies using human cancer cell lines treated with a cell permeable peptide that interferes with IQGAP1's ability to bind to PI3K, and *in vivo* studies utilizing mice genetically knocked out for the *Iqgap1* (*Iqgap1*$^{-/-}$). *In vivo* EGF-stimulation assays were used to evaluate PI3K signaling. To study the role of IQGAP1 in HNC, we used a well-validated mouse model that drives HNC via a synthetic oral carcinogen, 4-nitroquinoline 1-oxide (4NQO).

Results—IQGAP1 is necessary for efficient PI3K signaling *in vitro* and *in vivo*. Disruption of IQGAP1-scaffolded PI3K/AKT signaling reduced HNC cell survival. *Iqgap1*$^{-/-}$ mice had significantly lower cancer incidences, lesser disease severity and fewer cancer foci. IQGAP1 protein levels were increased in HNC arising in *Iqgap1+/+* mice. The level of PI3K signaling in 4NQO-induced HNC arising in *Iqgap1*$^{-/-}$ mice was significantly reduced, consistent with the hypothesis that IQGAP1 contributes to HNC at least partly through PI3K signaling. High IQGAP1 expression correlated with reduced survival, and high pS6 levels correlated with high IQGAP1 levels in HNC patients.

Conclusions—These data demonstrate that IQGAP1 contributes to head and neck carcinogenesis.

Corresponding author: Paul F. Lambert (plambert@wisc.edu).

Keywords

IQGAP1; head and neck carcinogenesis; PI3K pathway; signaling scaffolding; head and neck cancer mouse model

INTRODUCTION

Head and neck cancers (HNC), most often, squamous cell carcinoma, arise in the mouth/throat region and are the sixth most frequent cancer worldwide, with a 5-year survival rate less than 50% (1,2). Risk factors for HNC include smoking, alcohol abuse, and infection with high-risk human papillomaviruses (1). Epidermal growth factor receptor (EGFR) and downstream phosphoinositide 3-kinase (PI3K) signaling are among the most frequently altered factors in HNCs (3–7).

PI3K is implicated in diverse physiologic processes including cell survival, migration and proliferation. In response to agonists, PI3K converts phosphatidylinositol-4,5- biphosphate (PIP2) to phosphatidylinositol-3,4,5-trisphosphate (PIP3). PIP3 then functions as a messenger to activate AKT, which activates multiple downstream effectors including the mTOR1 pathway to promote cell growth and protein synthesis (8,9). PI3K/AKT/mTOR signaling plays an important role in HNC. Mutations in the PI3K pathway arise in 30% of HNCs (3). Activating mutations in the 110 kDa catalytic subunit of PI3K, are found in 20% of HNCs (5). These *PIK3CA* mutations increase PI3K activity and thereby promote HNC cell growth (3). Pan-PI3K inhibitors suppress HNC cell growth both in tissue culture and in xenografts (8,10,11). However, clinical treatment with small molecule inhibitors targeting the PI3K/AKT/mTOR pathway have had limited success due to toxicity and possible drug resistance (8). Therefore, drugs targeting other components of the PI3K/AKT/mTOR pathway in HNC may provide more effective treatments.

IQ motif-containing GTPase activating protein 1 (IQGAP1), a scaffolding protein and mediates many cellular pathways, contains multiple protein-interaction domains and interacts with over 100 proteins to regulate diverse cellular processes including cytoskeletal dynamics, adhesion, cell motility/invasion, and cell proliferation (12–16). It can also bind directly to EGFR and mediate receptor activation (17) as well as scaffold and facilitate the Ras-MAPK pathway (16). IQGAP1 is overexpressed in several cancers, including breast, lung, colorectal carcinomas and squamous cell carcinoma of head and neck (12,18–21). High levels of IQGAP1 are linked to poor prognosis in HNC (21). Diminished tumorigenesis was observed in *Iqgap1-knockout* mice in a Ras-driven skin cancer model (16).

IQGAP1-mediated PI3K/AKT/mTOR signaling is important for cancer cell survival. Recently, IQGAP1 was reported to assemble each of the kinases, including PI3K and AKT that are necessary for rapid, channeled conversion of PI to PIP3 upon receptor activation, resulting in increased AKT activation *in vitro* and *in vivo* (22). Cell permeable peptides that interfered with the ability of IQGAP1 to bind to PI3K disrupted the intracellular formation of the scaffolded PI3K complex and inhibited AKT activation (22). These peptides diminished breast cancer cell survival, including cell lines harboring *PIK3CA* mutations,

while not affecting normal cells (22). This data indicated IQGAP1-mediated PI3K signaling in cancer cell survival. Blocking IQGAP1-mediated PI3K signaling using the same peptide in UM-SCC47, a HNC cell line, inhibited cell proliferation, migration and invasion (23). Upon IQGAP1 overexpression, IQGAP1-dependent phosphorylation of ERK1/2 is impeded via AKT-mediated phosphorylation of Forkhead box protein O1, a downstream effector of AKT, suggesting that there is crosstalk among IQGAP1-mediated pathways (24).

Here, we focus on the role of IQGAP1 in HNC using a well-established mouse model for keratinizing squamous cell carcinoma of head and neck, in which a synthetic oral carcinogen, 4-nitroquinoline 1-oxide (4NQO), is used to drive tumorigenesis (25). This carcinogen causes a spectrum of DNA damage similar to that caused by tobacco-associated carcinogens (25). 4NQO is known to cause HNC in mice at least in part by activating EGFR signaling, upstream of the PI3K/AKT/mTOR pathway, and therefore was chosen as a preclinical model that closely reflects activation of EGFR in human HNCs (9,25).

To test the role of IQGAP1, we used genetically engineered mice deficient for IQGAP1 (16,26). These *Iqgap1-knockout (Iqgap1*$^{-/-}$) mice develop normally and have no apparent phenotypes (26). We observed a reduced level of PI3K signaling in *Iqgap1*$^{-/-}$ mice upon EGF stimulation. Upon treatment with 4NQO, we observed that loss of IQGAP1 reduced the incidence of carcinoma, the number of tumor foci and disease severity. In the absence of IQGAP1, PI3K signaling was significantly decreased in 4NQO-induced HNC. In *Iqgap1*$^{+/+}$ mice, IQGAP1 protein level was upregulated in HNC, consistent with that observed in human HNCs (20,21). Survival analysis using RNAseq data from The Cancer Genome Atlas program (TCGA) revealed that high expression of IQGAP1 correlates with poorer 5-year survival probabilities in HNC patients. We also discovered a positive correlation between levels of IQGAP1 and PI3K signaling that is statistically significant utilizing a tissue microarray (TMA). Our studies support the hypothesis that IQGAP1 functions as an oncogene in head and neck carcinogenesis, and does so at least in part by activating the PI3K/AKT signaling pathway.

MATERIALS AND METHODS

Cell culture and siRNA knockdown

UPCI-SCC90 cells were purchased from ATCC. UM-SCC1 cells were purchased from Millipore. Cal33 cells were gifts from Dr. Jennifer Grandis from University of California-San Francisco. All cells were maintained in DMEM supplemented with 10% fetal bovine serum (Gibco).

In the HNC cells, siRNAs targeting human IQGAP1 (Dharmacon, L-004694) or control siRNAs (Dharmacon, D-001810–10) were transfected using Lipofectamine RNAiMAX (Thermo Fisher Scientific) for 72 hours.

Peptide treatment and cell counting

IQ3 peptides were generated as previously described (22). The HNC cells were seeded on wells of 6-well culture dishes. Media were changed with or without IQ3 peptide added in the indicated concentrations every day for 3 days. For measuring cell viability, 50,000 cells were

seeded in each well. Once cells attached, scramble or 30 μM IQ3 peptides were treated for the indicated time. After peptide incubation, cells were lifted by Trypsin-EDTA (Thermo Fisher Scientific) and Trypan Blue-positive viable cells were counted using a hemocytometer. The experiments were independently repeated 3 times and the graphs were shown mean +/− standard deviation.

Mice

Iqgap1$^{+/+}$ and *Iqgap1*$^{-/-}$ mice (from Dr. David Sacks, National Institutions of Health) (16) were generated on a mixed genetic background (50%*FVB*/50%(*129+C57BL/6*)). All mice were genotyped by PCR as described previously (16). Mice were housed in the Association for Assessment of Laboratory Animal Care-approved McArdle Laboratory Animal Care Unit. All procedures were carried out in accordance with an animal protocol approved by the University of Wisconsin Institutional Animal Care and Use Committee.

In vivo EGF stimulation

Mice were treated with epidermal growth factor (EGF) as previously described (27). Briefly, 5-week old *Iqgap1*$^{+/+}$ and *Iqgap1*$^{-/-}$ mice were injected subcutaneously with 5 μg/g body weight of hEGF (Prospec, CYT-217), or phosphate-buffered saline (PBS) alone as vehicle control. hEGF was stored as 1 mg/mL stock solution in PBS at −80°C. Mice were sacrificed 10 minutes after injection and dorsal skin was harvested and snap frozen in liquid nitrogen.

Protein lysate preparation and immunoblotting

Cells were lysed with a lysis buffer (1% Brij58, 150 mM NaCl, 2 mM $CaCl_2$, 2 mM $MgCl_2$, 20 mM HEPES pH 7.4) and protein concentration was measured using BCA method (Thermo Fisher Scientific). Frozen skin was cut into small pieces on ice using razor blades, homogenized in 300 μL RIPA buffer (25mM Tris [pH 8], 150mM NaCl, 0.1%SDS, 0.5% sodium deoxycholate, 1%Triton X-100) with protease and phosphatase inhibitors using a plastic pestle (Axygen), and incubated on an orbital shaker at 4°C for 20 minutes. Homogenates were centrifuged at 14,000 rpm for 20 minutes at 4°C, and supernatants (protein lysates) collected. Protein concentrations were determined using the Bradford Protein Assay (Bio-Rad). Equivalent amounts of protein were resolved on precast Mini-PROTEAN TGX 7.5% gels (Bio-Rad) and transferred to PVDF membranes (Millipore). Membranes were blocked with 5% nonfat dry milk in TBST (Tris-buffered saline with 0.1% Tween-20). Primary antibodies used were summarized in Supplementary Table 1. Horseradish peroxidase-conjugated secondary antibodies (1:10,000) (Jackson ImmunoResearch) and chemiluminescent substrates (Clarity ECL Substrates; Bio-Rad) were used to visualize on a Bio-Rad ChemiDoc Imaging System.

4NQO induced head and neck carcinogenesis study

6–8 weeks old *Iqgap1*$^{+/+}$ and *Iqgap1*$^{-/-}$ mice were treated with 4NQO (Sigma) in their drinking water at a concentration of 100 μg/ml or 20 μg/ml (stored at 4°C as a 5 mg/mL stock) for 16 weeks. Mice were then returned to normal drinking water for 5 (with 100 μg/ml 4NQO) or 8 weeks (with 20 μg/ml 4NQO). At the end of this period, mice were

euthanized, grossly visible, overt tumors on the tongue and esophagus were quantified, and tissues were collected for histological analysis.

Histological analysis

The tongue and esophagus were harvested and fixed in 4% paraformaldehyde (in PBS) for 24 hours, then switched to 70% ethanol for 24 hours, processed, embedded in paraffin, and sectioned at 5 μm intervals. Every 10^{th} section was stained with hematoxylin and eosin and examined by pathologist Dr. Buehler in a blinded fashion for severest state of neoplasia.

Immunofluorescence

Tissue sections were deparaffinized in xylenes and rehydrated in 100%, 95%, 70% and 50% ethanol then in water. Antigen unmasking was performed by heating with 10 mM citrate buffer (pH=6) for 20 minutes. Blocking was performed with Superblock blocking buffer (ThermoFisher) for 1 hour at room temperature (RT). Slides were incubated in primary antibody at 4°C, overnight in a humidified chamber. Alexa goat-anti-rabbit-594 (Invitrogen, 1:500) was applied the next day for 1 hour at RT. Sections were counterstained with DAPI and mounted in Prolong Diamond Antifade Mountant (Invitrogen). All images were taken with a Zeiss AxioImager M2 microscope using AxioVision software version 4.8.2.

pERK signals were detected using a tyramide-based signal amplification (TSA) method (28) as previously described (29). Tissues were incubated in anti-pERK (1:100) at 4°C, overnight and then 1 hour in Goat-anti-rabbit-HRP secondary antibody at 1:500 dilution in blocking buffer at RT the next day. TSA was then performed, followed by incubation with anti-streptavidin-647 (Invitrogen,1:500) for 1 hour at RT. Sections were counterstained and mounted.

Image analysis and statistical analysis

One-sided T-tests were used to determine the significance of AKT, ERK and S6 activation upon *in vivo* EGF stimulation. The %activated protein was calculated by comparing the ratio of phosphorylated protein signal to total protein signal in both PBS-injected (control) and EGF-injected (stimulated) mice. Protein activation was then calculated by determining the fold change of %activated protein between EGF/PBS treated mice. Error bars (standard deviation) were calculated by taking the average of 4 or 6 replicates.

To compare overt tumor incidences and overall cancer incidence among groups, a two-sided Fisher exact test was performed using MSTAT statistical software version 6.4.2 (http://www.mcardle.wisc.edu/mstat). Wilcoxon rank sum test was performed to determine the significance of differences in number of overt tumor foci and total cancer foci using MSTAT. For disease severity, each microscopic tumor grade was assigned a ranking order (mild dysplasia= 1, moderate dysplasia= 2, severe dysplasia/carcinoma in situ= 3, well-differentiated invasive carcinoma= 4, moderately-differentiated invasive carcinoma= 5 and poorly differentiated invasive carcinoma= 6) and analyzed using the Wilcoxon rank sum test.

To quantify pS6 and pERK levels between groups of mice, 10 immunofluorescence microscopic images (200X) of regions of the normal and cancer tissue per mouse were

captured. All images were taken under constant exposure time. Images were processed using ImageJ software version 10.2 (NIH, Bethesda, MD). pS6 and pERK levels on each image were calculated by integrated intensity of the signal, normalized to the DAPI signal from the same area. For statistical analysis, pS6 and pERK levels in the normal and cancer tissue were calculated separately by taking the average levels in each of the corresponding 10 images per mouse, and the data was pooled across replicates. A two-sided T-test was used to determine the significance of signal differences between groups.

TCGA survival analysis

TCGA RNA-seq data was accessed through the Human Protein Atlas website (https://www.proteinatlas.org/ENSG00000140575-IQGAP1/pathology/tissue/head+and+neck+cancer). Cutoff for IQGAP1 levels was suggested by the database as shown on the website. Only data for the first 5 years was analyzed due to the smaller number of censored subjects. Kaplain-Meier survival curve analysis and Logrank test were done using MSTAT.

Tissue Microarray Analysis

HNC TMA slide was provided by the Wisconsin Head and Neck Cancer SPORE. The TMA slide contains 411 cores collected from 137 patient specimens, including 180 primary, 153 recurrent, and 78 metastasized cancer cores. About 10% of sample cores were lost during sectioning and staining. Remaining 360 cores from 124 patients were analyzed. Within these 360 cores, there are 168 p16-positive, 162 p16-negative, and 30 p16-equivocal cores. p16 is the indicator for HPV status in clinics.

Multiplex staining on the TMA slide was carried out to measure DAPI, pS6, IQGAP1, and pan-cytoskeleton. The slide was stained sequentially. Day1: same as in the previously described TSA method, with anti-pS6 antibody overnight at 4°C. Day2: same secondary antibody and TSA incubation as described. Then the slide was probed overnight with both anti-IQGAP1 and anti-pan-cytokeratin. Day3: the slide was incubated in a cocktail of fluorescent secondary antibodies at 1:200 dilution at RT for 1hr, using anti-streptavidin-488 (Invitrogen, reading pS6), goat-anti-rabbit-546 (reading IQGAP1), and goat-anti-mouse-647 (reading pan-cytokeratin). The slide was then counterstained with DAPI and mounted. The stained TMA was scanned by the UW Translational Research Initiatives in Pathology (TRIP) facility using the Vectra multispectral imaging system at 20X. The acquired images were analyzed by the Perkin-Elmer inForm™ software, which identifies epithelia with pan-cytokeratin patterns, and individual cells with DAPI staining. Only signals from certain cell compartments (cytoplastic pS6 and membrane IQGAP1) in identified cells from epithelium was quantified. The expression levels of both markers were quantified and reported as H-scores. Spearman Rank Correlation test against these H-scores from both markers was conducted using MSTAT.

RESULTS

IQGAP1 is necessary for efficient PI3K signaling *in vitro* and *in vivo*

Prior studies demonstrated that IQGAP1 scaffolds the PI3K signaling pathway (22), and blocking IQGAP1-mediated PI3K signaling reduced cell proliferation, migration and

invasion in UM-SCC47 cells(23). Because UM-SCC47 has no known mutation in PI3K signaling pathway (30), we tested the role of IQGAP1 and its PI3K-scaffolding ability in 3 additional HNC cell lines: UPCI:SCC-90 (SCC-90, *PTEN* mutation), Cal33 (*PIK3CA* mutation), and UM-SCC1 (SCC-1) (30,31). Knockdown of IQGAP1 led to reduced PI3K signaling in these cells (Figure 1A). We then tested whether IQGAP1-mediated PI3K signaling is required for growth/ survival of these HNC cell lines. Treatment with the cell permeable IQ3 peptide, which inhibits IQGAP1's ability to bind to PI3K, led to reduced PI3K signaling (Figure 1B) and inhibited cell growth/survival of all cell lines (Figure 1C). Thus, IQGAP1 contributes to the PI3K signaling pathway in cancer cells, and IQGAP1-mediated PI3K signaling is necessary for HNC cell growth/survival.

To assess whether IQGAP1 is necessary for activation of PI3K/AKT pathway signaling *in vivo*, we utilized *Iqgap1-knockout* mice ($Iqgap1^{-/-}$) (Supplementary Figure 1A) (26). PI3K signaling can be activated *in vivo* via EGF stimulation (27). Activation of the PI3K/AKT pathway by EGF was scored as the ratio of pAKT/AKT and pS6/S6. We found that AKT activation upon EGF stimulation was significantly lower in $Iqgap1^{-/-}$ mice compared to $Iqgap1^{+/+}$ mice (p=0.006, T-test, one-sided) (Figure 1D–E). We also observed a significantly lower S6 activation in $Iqgap1^{-/-}$ mice compared to $Iqgap1^{+/+}$ mice (p=0.038) (Figure 1D,F). These data indicated that IQGAP1 is required for efficient activation of PI3K signaling upon EGF stimulation. Previous studies suggested that IQGAP1 scaffolds the Ras-MAPK signaling pathway (16,32), another important pathway implicated in various epithelial cancers that can also be activated by EGF. We found that $Iqgap1^{-/-}$ mice did not display significantly different levels of ERK activation than $Iqgap1^{+/+}$ mice (Supplementary Figure 1B–C).

IQGAP1 contributes to overt head and neck tumorigenesis *in vivo*

As shown above, IQGAP1 is necessary both *in vitro* and *in vivo* for efficient PI3K/AKT signaling. This pathway is often activated in HNC (5), and disruption of IQGAP1-mediated PI3K signaling by the IQ3 peptide decreased HNC cell survival (Figure 1B–C). Therefore, we next tested whether loss of IQGAP1 prevents or reduces the onset and/or severity of HNC using a well-established mouse model for keratinizing squamous cell carcinoma of the head and neck (25). Groups of $Iqgap1^{+/+}$ and $Iqgap1^{-/-}$ mice were given 4NQO, the synthetic oral carcinogen, in their drinking water for 16 weeks, followed by 5 or 8 weeks of normal drinking water (Figure 2A). Mouse weight was used as a criterion to monitor mouse health. With 100 μg/ml 4NQO, morbidity issues, as reflected by weight loss, arose in a few $Iqgap1^{+/+}$ mice by week 16, the end-point of 4NQO treatment, and worsened as the experiment proceeded. Interestingly, no weight loss was evident in the $Iqgap1^{-/-}$ group of mice. We ended the 100 μg/ml dosage study early, at 21 weeks instead of 24 weeks, because more than 20% of $Iqgap1^{+/+}$ mice showed significant weight loss. With 20 μg/ml 4NQO, no significant morbidity issues were observed.

Both groups developed tongue and esophageal overt tumors in all animals when treated with 100 μg/ml 4NQO. When treated with 20 μg/ml 4NQO, $Iqgap1^{-/-}$ mice showed lower, though not significant, overt tumor incidence compared to $Iqgap1^{+/+}$ mice (82% vs. 61%, Figure 2B). $Iqgap1^{-/-}$ mice also had fewer overt tumors per mouse compared to $Iqgap1^{+/+}$

mice (Figure 2C). While this difference was not significant with 100 μg/ml of 4NQO, *Iqgap1*$^{-/-}$ mice treated with 20 μg/ml of 4NQO developed significantly fewer overt tumors per mouse than *Iqgap1*$^{+/+}$ mice (mean: 2.68 vs. 1.57, p=0.05, Wilcoxon rank sum test, two-sided). Together, these overt tumor data demonstrate that IQGAP1 contributes to tumorigenesis in the head and neck region *in vivo*.

IQGAP1 contributes to the frequency and severity of invasive squamous cell carcinoma

We next assessed disease severity in both the tongue and esophageal cancers by histopathologic grading of dysplasia and invasive carcinoma (Table 1). When treated with 100 μg/ml 4NQO, 68.4% of *Iqgap1*$^{+/+}$ mice and 62.5% of *Iqgap1*$^{-/-}$ mice developed invasive carcinoma, while treated with 20 μg/ml 4NQO, *Iqgap1*$^{+/+}$ mice developed significantly higher incidence of invasive carcinoma than *Iqgap1*$^{-/-}$ mice (73% vs. 39%, p<0.05, Fisher's exact test, two-sided, Figure 3A), indicating that IQGAP1 affects the overall percentage of mice developing cancer. *Iqgap1*$^{+/+}$ mice also developed overall significantly more high-grade tumors than *Iqgap1*$^{-/-}$ mice in both treatment groups (Table 1), demonstrating that IQGAP1 contributes to increased disease severity upon 4NQO treatment *in vivo*.

To test whether there is any gender-specific differences in the effect of IQGAP1 on head and neck disease severity, a detailed breakdown of disease severity depending on gender is summarized in Supplementary Figure 2A. In mice treated with 100 μg/ml 4NQO, no difference was observed between females and males in either experiment groups. In mice treated with 20 μg/ml 4NQO, female mice in both genotypes developed slightly more severe disease than male mice, though neither reached significance. With the loss of IQGAP1, females demonstrated a higher cancer incidence than males, though again the difference did not reach statistical significance (Supplementary Figure 2B).

To test whether there is any site-specific differences in the effect of IQGAP1 on head and neck disease severity, we compared the disease severity depending on tumor-arising sites, esophagus or tongue (Supplementary Figure 3A). When treated with 100 μg/ml 4NQO, *Iqgap1*$^{-/-}$ mice developed slightly less severe disease than *Iqgap1*$^{+/+}$ mice in both esophagus and tongue, though neither reached significance. When treated with 20 μg/ml 4NQO, *Iqgap1*$^{-/-}$ mice developed significantly less severe disease than *Iqgap1*$^{+/+}$ mice in the tongue (mean 2.8 vs.1.8, p=0.03, Wilcoxon, two-sided). The same trend was observed in the esophagus, though not reached significance. When we compared the cancer incidence on both sites, *Iqgap1*$^{-/-}$ mice showed lower cancer incidence, though not significant, than *Iqgap1*$^{+/+}$ mice when treated with 100 μg/ml 4NQO (Supplementary Figure 3B). When treated with 20 μg/ml 4NQO, *Iqgap1*$^{-/-}$ mice demonstrated significantly lower cancer incidence than *Iqgap1*$^{+/+}$ mice in the esophagus (p=0.04, Fisher exact, two-sided). The same trend was observed in the tongue with a difference that approached significance (Supplementary Figure 3B).

We then assessed the multiplicity of cancer foci and found that, *Iqgap1*$^{+/+}$ mice treated with 100 μg/ml 4NQO developed significantly higher numbers of cancer foci per mouse compared to like-treated *Iqgap1*$^{-/-}$ mice (Figure 3B, mean: 2.3 vs. 1.09, p<0.001, Wilcoxon, two-sided). We also observed that with the same treatment, *Iqgap1*$^{+/+}$ mice developed

significantly higher numbers of poorly-differentiated, high-grade cancer compared to the *Iqgap1*$^{-/-}$ mice, which developed mostly well-differentiated, low-grade cancer foci (Figure 3C, mean: 6.13 vs. 5.09, p<0.001, Wilcoxon, two-sided). In mice treated with 20 μg/mL 4NQO, the same trends for both number of cancer foci and cancer grade were observed between *Iqgap1*$^{+/+}$ and *Iqgap1*$^{-/-}$ mice, though the differences did not reach statistical significance. These data further demonstrate that IQGAP1 contributes to head and neck carcinogenesis.

IQGAP1 protein levels are upregulated in HNC

IQGAP1 is overexpressed in many human cancers (12,20,21,33,34). We therefore looked at levels of IQGAP1 protein in our 4NQO-induced HNC model by immunofluorescence. Higher levels of IQGAP1 protein were detected in cancer tissue compared to normal tissue of both the tongue and the esophagus of *Iqgap1*$^{+/+}$ mice (Figure 4A, Supplementary Figure 1A). The upregulation of IQGAP1 in 4NQO-induced HNC in mice is consistent with prior studies reporting overexpression of IQGAP1 in HNC patients (20,21).

PI3K signaling is downregulated in IQGAP1-null mice at tumor sites

IQGAP1 regulate diverse cellular pathways including scaffolding and facilitating Ras-MAPK pathway and PI3K-AKT pathways, and promoting Wnt signaling by enhancing nuclear localization of β-catenin, etc. (13,15,16,22). We wanted to determine which pathways contributed to IQGAP1-mediated head and neck carcinogenesis. Given that the 4NQO HNC mouse model is an EGFR-driven cancer model (25), in addition to previous data showing that PI3K signaling decreased in the absence of IQGAP1, we evaluated whether PI3K signaling decreases in *Iqgap1*$^{-/-}$ experimental mice. In the esophagus, the 4NQO-induced cancers arising in the *Iqgap1*$^{-/-}$ mice had a significantly lower level of pS6 than the cancers arising in the *Iqgap1*$^{+/+}$ mice (Figure 4B, p=0.02, T test, two-sided). The data is consistent with the hypothesis that IQGAP1 contributes to 4NQO-induced HNC by driving PI3K signaling. However, IQGAP1 status did not correlate significantly with pS6 levels in tongue cancers (Supplementary Figure 3), suggesting that IQGAP1 may exhibit tissue-specific differences in pathway modulation in promoting HNC.

ERK signaling significantly decreases in 4NQO-induced tumors, independent of IQGAP1 status

Our data demonstrates that levels of ERK activation upon EGF stimulation *in vivo* was not significantly changed in the presence or absence of IQGAP1 (Supplementary Figure 1B–C). However, because previously suggested role for IQGAP1-scaffolded Ras-MAPK in cancer development (16,32,35,36), we decided to examine the ERK signaling levels in our 4NQO-induced HNCs. In the esophageal carcinomas, ERK signaling was significantly reduced in 4NQO-induced HNCs, regardless of IQGAP1 status (p=0.004<0.05, T-test, two-sided) (Supplementary Figure 1D–E). There was no significant difference in pERK levels in tumor and normal tissue between *Iqgap1*$^{+/+}$ and *Iqgap1*$^{-/-}$ mice (normal: p=0.71; tumor: p=0.06, T-test, two-sided) (Supplementary Figure 1F). These data indicate that IQGAP1 may not contribute to HNC through ERK signaling.

High expression of IQGAP1 correlates with poorer survival in HNC patients

Previous research using human HNC tissue microarrays (TMAs) demonstrated that high levels of IQGAP1 protein correlates with poor survival in HNC patients (21). To further study the relationship between IQGAP1 and HNC patient survival, we analyzed RNA-seq data generated by TCGA. IQGAP1 transcript levels in patient samples were reported as median FPKM (number fragments per kilobase of exon per million reads). Using a Kaplan-Meier survival curve analysis, we found that HNC patients with high levels of IQGAP1 mRNA were associated with a significantly lower 5-year survival probability in HNC patients (Figure 5A, $p<0.001$, Logrank test, two sided).

Levels of IQGAP1 positively correlate with levels of PI3K signaling in HNC patient samples

With the knowledge that IQGAP1 correlates with HNC patient survival, we investigated whether the levels of IQGAP1 correlates with PI3K signaling in an HNC TMA. The levels of IQGAP1 and pS6 were reported as H-scores. Because our study did not involve HPV, we focused on p16-negative samples. Using a Spearman Rank Correlation test, we observed a positive correlation between IQGAP1 and pS6, with a coefficient rho=0.28, which was highly significant ($p<0.001$, Figure 5B, Supplementary Figure 5).

We were also interested in whether levels of IQGAP1 correlate with responses to PI3K signaling inhibitors. We obtained 5 patient-derived xenografts (PDXs) samples that were previously tested for response to a mTORC inhibitor, AZD8055 (31). 4 of these PDXs, UWSCC1, UWSCC6, UWSCC17 and UWSCC64, were sensitive to the inhibitor, while UWSCC13 was resistant to the inhibitor (31). We observed that the IQGAP1 levels varied a lot within these 5 PDXs and did not demonstrate any pattern correlating with the responses to the inhibitor (Supplementary Figure 6). Analysis of a larger cohort may be necessary to determine whether the IQGAP1 levels correlate with response to PI3K signaling pathway inhibitors.

DISCUSSION

In this report, we demonstrate that IQGAP1 is necessary for growth/survival of human HNC cells *in vitro*, and contributes to the incidence and severity of HNC disease in an *in vivo* mouse model of head and neck keratinizing squamous cell carcinoma. Specifically, knockdown of IQGAP1 reduced PI3K signaling in HNC cells. Likewise, IQGAP1 was necessary for efficient PI3K signaling *in vivo*. Disruption of IQGAP1-mediated PI3K signaling by a cell permeable peptide inhibited HNC cell survival. Utilizing the 4NQO-induced HNC model that is dependent upon EGFR signaling, we observed that *Iqgap1*$^{-/-}$ mice showed fewer cancer foci, less cancer incidence and less overall head and neck disease severity, providing compelling evidence that IQGAP1 contributes to HNC *in vivo*. IQGAP1 protein levels were upregulated in cancer foci in both the tongue and esophagus of 4NQO-treated *Iqgap1*$^{+/+}$ mice, consistent with what is seen in human HNC. PI3K signaling in the 4NQO-induced esophageal cancers was downregulated in the *Iqgap1*$^{-/-}$ mice compared to *Iqgap1*$^{+/+}$ mice, consistent with the hypothesis that IQGAP1 is acting through PI3K signaling to promote HNC. Analysis of TCGA RNA-seq data demonstrated that high levels

of IQGAP1 significantly correlates with poor 5-year survival in HNC patients. A positive correlation between IQGAP1 and PI3K signaling also was observed using an HNC TMA.

Upon 4NQO treatment, esophageal PI3K signaling in *Iqgap1*$^{-/-}$ mice was significantly lower in cancer sites when compared to *Iqgap1*$^{+/+}$ mice, supporting that IQGAP1 promotes HNC by driving PI3K signaling, given that IQGAP1 scaffolds PI3K signaling (22). However, no significant difference was observed for PI3K signaling in tongue (Supplementary Figure 4), suggesting that there may be site-specific differences in how IQGAP1 contributes to HNC. This is supported by the differences of disease severity and cancer incidences between the two genotypes of mice in esophagus and tongue (Supplementary Figure 3). Upon 20 μg/ml 4NQO, with the loss of IQGAP1, we observed a significant decrease in overall disease severity in tongue but not in esophagus (Supplementary Figure 3A), meanwhile a significantly reduced cancer incidence in esophagus but not in tongue (Supplementary Figure 3B). A hypothesis for these observations is that, in the tongue of *Iqgap1*$^{-/-}$ mice, another factor(s) acts to maintain signaling when IQGAP1 is absent. One candidate for this other factor is IQGAP3, another member of the IQGAP family that has highly homologous structural motifs to IQGAP1 (37,38). IQGAP3 functions similarly to IQGAP1, including its interactions with Rac1 and Cdc42 for actin filament regulation, and promotes the Ras/ERK signaling (37,39,40). Interestingly, when IQGAP1 was knocked down in human hepatocellular cancer cells, levels of IQGAP3 protein increased (41). Although it is still unknown whether IQGAP3 scaffolds for PI3K signaling, it is possible that under certain circumstances, IQGAP3 compensates and maintains PI3K signaling when IQGAP1 is absent. However, our own data do not currently support this hypothesis. In mouse skin lysates, we observed a significant increase in levels of IQGAP3 protein with the loss of IQGAP1 in female mice, but not in male mice ($p<0.001$, T-test, two-sided) (Supplementary Figure 7A–B). *Iqgap1*$^{-/-}$ female mice had significantly higher levels of IQGAP3 than *Iqgap1*$^{-/-}$ male mice ($p<0.001$, T-test, two-sided) (Supplementary Figure 7C). Nevertheless, we did not see a significant difference in disease severity or cancer incidence in the head and neck region between female and male mice in either the *Iqgap1*$^{+/+}$ or *Iqgap1*$^{-/-}$ context (Supplementary Figure 2). This finding raises a question as to whether IQGAP3 compensates for IQGAP1 in carcinogenesis in an epithelial context.

Although we have focused on IQGAP1-mediated PI3K signaling, we cannot discount the possibility that IQGAP1 may act through other pathways to promote HNC. *Jameson et. al.* proposed that, in a Ras-driven skin cancer model, *Iqgap1*$^{-/-}$ mice were resistant to skin tumorigenesis, and this reduced tumorigenesis was due to the lack of IQGAP1-scaffolded Ras-MAPK signaling (16). In our study, we observed a significant reduction in Ras-MAPK signaling, in HNC, but this was regardless of IQGAP1 status, which indicates that IQGAP1-mediated Ras-MAPK signaling is not driving HNC in our model (Supplementary Figure 1). Multiple studies have also linked IQGAP1 with Wnt/ β-catenin signaling in cancer promotion (42–44). IQGAP1 is required for sufficient R-spondin-induced Wnt/β-catenin signaling (44). In thyroid cancer, knockdown of IQGAP1 reduced Wnt/β-catenin signaling both *in vitro* and *in vivo*, inhibiting tumor growth and epithelial mesenchymal transition(43). In a hepatocellular carcinoma cell line, IQGAP1 co-immunoprecipitated with β-catenin, increased β-catenin expression and nuclear β-catenin level, and activated downstream transcription (42). In fact, increased levels of nuclear β-catenin were observed in a subset of

HNCs (45). We envisage using, in the future, an unbiased proteomic approach to better understand what signaling pathways are altered in IQGAP1-null tissue.

Because the *Iqgap1* gene was deactivated in all cell types in *Iqgap1*$^{-/-}$ mice, we cannot rule out the possibility that the reduced cancer phenotypes observed in *Iqgap1*$^{-/-}$ mice were due to the IQGAP1's involvement in mediating immune responses. IQGAP1 has been implicated in regulating immune cells functions. IQGAP1-deficient T cells were shown to have enhanced T-Cell receptor-mediated signaling and increased cytokine production (46). Primary and naïve CD8+ T cells isolated from *Iqgap1*$^{-/-}$ mice showed increased levels of cytokine production upon stimulation (47). However, IQGAP1 seems to have different roles in other types immune cells. Loss of IQGAP1 diminished the cytotoxic activity of a Natural Killer(NK) -like cell line (48). IQGAP1 also mediates NK cell activation and anti-tumor responses *in vivo* (49). In macrophages, IQGAP1 is involved in the phagocytosis and the activation of caspase-1 upon infection (50–52). The exact role of IQGAP1 in mediating immune response in the context of HNC remains unclear at this point.

Overall, this study demonstrates that IQGAP1 contributes to HNC, and at least in part through PI3K signaling. This is the first time that IQGAP1 is shown to promote HNC in an *in vivo* model. By understanding how IQGAP1 contributes to HNC, we may identify new drug targets that mediate IQGAP1-mediated oncogenicity, providing new therapies to treat patients with HNCs.

Supplementary Material

Refer to Web version on PubMed Central for supplementary material.

ACKNOWLEDGEMENTS

This study was supported by the following NIH grants: CA210807, CA022443, DE026787. This study made use of core facilities of the University of Wisconsin Carbone Cancer Center (NIH grant CA014520). We wish to thank Professor Alan Rapraeger as well as other members of the Lambert lab for useful discussions.

The author(s) thank the University of Wisconsin Translational Research Initiatives in Pathology laboratory (TRIP), supported by the UW Department of Pathology and Laboratory Medicine, UWCCC (P30 CA014520) and the Office of The Director- NIH (S10OD023526) for use of its facilities and services.

The TMA analysis was supported by the Specialized Program of Research Excellence (SPORE) program, through the NIH National Institute for Dental and Craniofacial Research (NIDCR) and National Cancer Institute (NCI), grant P50DE026787. The content is solely the responsibility of the authors and does not necessarily represent the official views of the NIH.

REFERENCES CITED

1. Siegel RL, Miller KD, Jemal A. Cancer statistics, 2017. CA Cancer J Clin [Internet]. 2017 [cited 2018 Dec 12];67:7–30. Available from: http://www.ncbi.nlm.nih.gov/pubmed/28055103 [PubMed: 28055103]
2. American Cancer Society. Cancer Facts & Figures 2017 [Internet]. Atlanta; 2017. Available from: https://www.cancer.org/content/dam/cancer-org/research/cancer-facts-and-statistics/annual-cancer-facts-and-figures/2017/cancer-facts-and-figures-2017.pdf
3. Lui VWY, Hedberg ML, Li H, Vangara BS, Pendleton K, Zeng Y, et al. Frequent Mutation of the PI3K Pathway in Head and Neck Cancer Defines Predictive Biomarkers. Cancer Discov [Internet].

2013 [cited 2018 Dec 3];3:761–9. Available from: http://www.ncbi.nlm.nih.gov/pubmed/23619167 [PubMed: 23619167]

4. Stransky N, Egloff AM, Tward AD, Kostic AD, Cibulskis K, Sivachenko A, et al. The Mutational Landscape of Head and Neck Squamous Cell Carcinoma. Science (80-) [Internet]. 2011 [cited 2018 Dec 3];333:1157–60. Available from: http://www.ncbi.nlm.nih.gov/pubmed/21798893
5. Cancer Genome Atlas Network. Comprehensive genomic characterization of head and neck squamous cell carcinomas. Nature [Internet]. 2015 [cited 2018 Dec 3];517:576–82. Available from: http://www.ncbi.nlm.nih.gov/pubmed/25631445 [PubMed: 25631445]
6. Agrawal N, Frederick MJ, Pickering CR, Bettegowda C, Chang K, Li RJ, et al. Exome Sequencing of Head and Neck Squamous Cell Carcinoma Reveals Inactivating Mutations in NOTCH1. Science (80-) [Internet]. 2011 [cited 2018 Dec 3];333:1154–7. Available from: http://www.ncbi.nlm.nih.gov/pubmed/21798897
7. Grandis JR, Tweardy DJ. Elevated levels of transforming growth factor alpha and epidermal growth factor receptor messenger RNA are early markers of carcinogenesis in head and neck cancer. Cancer Res [Internet]. 1993 [cited 2018 Dec 3];53:3579–84. Available from: http://www.ncbi.nlm.nih.gov/pubmed/8339264 [PubMed: 8339264]
8. Simpson DR, Mell LK, Cohen EEW. Targeting the PI3K/AKT/mTOR pathway in squamous cell carcinoma of the head and neck. Oral Oncol [Internet]. 2015 [cited 2019 Mar 10];51:291–8. Available from: http://www.ncbi.nlm.nih.gov/pubmed/25532816 [PubMed: 25532816]
9. Czerninski R, Amornphimoltham P, Patel V, Molinolo AA, Gutkind JS. Targeting mammalian target of rapamycin by rapamycin prevents tumor progression in an oral-specific chemical carcinogenesis model. Cancer Prev Res (Phila) [Internet]. 2009 [cited 2019 Mar 10];2:27–36. Available from: http://cancerpreventionresearch.aacrjournals.org/cgi/doi/10.1158/1940-6207.CAPR-08-0147 [PubMed: 19139015]
10. Erlich RB, Kherrouche Z, Rickwood D, Endo-Munoz L, Cameron S, Dahler A, et al. Preclinical evaluation of dual PI3K-mTOR inhibitors and histone deacetylase inhibitors in head and neck squamous cell carcinoma. Br J Cancer [Internet]. 2012 [cited 2019 Mar 10];106:107–15. Available from: http://www.nature.com/articles/bjc2011495 [PubMed: 22116303]
11. Keysar SB, Astling DP, Anderson RT, Vogler BW, Bowles DW, Morton JJ, et al. A patient tumor transplant model of squamous cell cancer identifies PI3K inhibitors as candidate therapeutics in defined molecular bins. Mol Oncol [Internet]. 2013 [cited 2019 Mar 10];7:776–90. Available from: http://doi.wiley.com/10.1016/j.molonc.2013.03.004 [PubMed: 23607916]
12. White CD, Brown MD, Sacks DB. IQGAPs in cancer: A family of scaffold proteins underlying tumorigenesis. FEBS Lett. 2009.
13. Goto T, Sato A, Adachi S, Iemura SI, Natsume T, Shibuya H. IQGAP1 protein regulates nuclear localization of β-Catenin via importin-β5 protein in wnt signaling. J Biol Chem. 2013;
14. Wang J-B, Sonn R, Tekletsadik YK, Samorodnitsky D, Osman MA. IQGAP1 regulates cell proliferation through a novel CDC42-mTOR pathway. J Cell Sci. 2009;
15. Smith JM, Hedman AC, Sacks DB. IQGAPs choreograph cellular signaling from the membrane to the nucleus. Trends Cell Biol. 2015.
16. Jameson KL, Mazur PK, Zehnder AM, Zhang J, Zarnegar B, Sage J, et al. IQGAP1 scaffold-kinase interaction blockade selectively targets RAS-MAP kinase-driven tumors. Nat Med. 2013;
17. McNulty DE, Li Z, White CD, Sacks DB, Annan RS. MAPK scaffold IQGAP1 binds the EGF receptor and modulates its activation. J Biol Chem [Internet]. 2011 [cited 2019 Jan 21];286:15010–21. Available from: http://www.jbc.org/lookup/doi/10.1074/jbc.M111.227694 [PubMed: 21349850]
18. Johnson M, Sharma M, Henderson BR. IQGAP1 regulation and roles in cancer. Cell Signal [Internet]. Pergamon; 2009 [cited 2019 Mar 18];21:1471–8. Available from: https://www-sciencedirect-com.ezproxy.library.wisc.edu/science/article/pii/S0898656809001016 [PubMed: 19269319]
19. Baker H, Patel V, Molinolo AA, Shillitoe EJ, Ensley JF, Yoo GH, et al. Proteome-wide analysis of head and neck squamous cell carcinomas using laser-capture microdissection and tandem mass spectrometry. Oral Oncol [Internet]. Pergamon; 2005 [cited 2019 Mar 18];41:183–99. Available

from: https://www-sciencedirect-com.ezproxy.library.wisc.edu/science/article/pii/S1368837504001903 [PubMed: 15695121]

20. Patel V, Hood BL, Molinolo AA, Lee NH, Conrads TP, Braisted JC, et al. Proteomic analysis of laser-captured paraffin-embedded tissues: a molecular portrait of head and neck cancer progression. Clin Cancer Res [Internet]. 2008 [cited 2019 Mar 6];14:1002–14. Available from: http://clincancerres.aacrjournals.org/cgi/doi/10.1158/1078-0432.CCR-07-1497 [PubMed: 18281532]
21. Wu C-C, Li H, Xiao Y, Yang L-L, Chen L, Deng W-W, et al. Over-expression of IQGAP1 indicates poor prognosis in head and neck squamous cell carcinoma. J Mol Histol [Internet]. 2018 [cited 2019 Jan 26];49:389–98. Available from: http://www.ncbi.nlm.nih.gov/pubmed/29846864 [PubMed: 29846864]
22. Choi S, Hedman AC, Sayedyahossein S, Thapa N, Sacks DB, Anderson RA. Agonist-stimulated phosphatidylinositol- 3,4,5-trisphosphate generation by scaffolded phosphoinositide kinases. Nat Cell Biol [Internet]. 2016 [cited 2017 Jul 5];18:1324–35. Available from: http://www.nature.com.ezproxy.library.wisc.edu/ncb/journal/v18/n12/pdf/ncb3441.pdf [PubMed: 27870828]
23. Chen M, Choi S, Jung O, Wen T, Baum C, Thapa N, et al. The Specificity of EGF-Stimulated IQGAP1 Scaffold Towards the PI3K-Akt Pathway is Defined by the IQ3 motif. Sci Rep [Internet]. 2019 [cited 2019 Aug 7];9:9126 Available from: http://www.ncbi.nlm.nih.gov/pubmed/31235839 [PubMed: 31235839]
24. Pan C-W, Jin X, Zhao Y, Pan Y, Yang J, Karnes RJ, et al. AKT-phosphorylated FOXO1 suppresses ERK activation and chemoresistance by disrupting IQGAP1-MAPK interaction. EMBO J [Internet]. 2017 [cited 2019 Mar 10];36:995–1010. Available from: http://emboj.embopress.org/lookup/doi/10.15252/embj.201695534 [PubMed: 28279977]
25. Tang X, Knudsen B, Bemis D, Tickoo S, Gudas LJ. Oral Cavity and Esophageal Carcinogenesis Modeled in Carcinogen-treated Mice. Clin Cancer Res [Internet]. 2003 [cited 2017 Jul 4];10:301–13. Available from: http://clincancerres.aacrjournals.org/content/clincanres/10/1/301.full.pdf
26. Li S, Wang Q, Chakladar A, Bronson RT, Bernards A. Gastric Hyperplasia in Mice Lacking the Putative Cdc42 Effector IQGAP1. 2000 [cited 2017 Jul 3];20:697–701. Available from: http://mcb.asm.org/content/20/2/697.full.pdf
27. Genther Williams SM, Disbrow GL, Schlegel R, Lee D, Threadgill DW, Lambert PF. Requirement of epidermal growth factor receptor for hyperplasia induced by E5, a high-risk human papillomavirus oncogene. Cancer Res [Internet]. 2005 [cited 2019 Jan 23];65:6534–42. Available from: http://cancerres.aacrjournals.org/lookup/doi/10.1158/0008-5472.CAN-05-0083 [PubMed: 16061632]
28. Hopman AHN, Ramaekers FCS, Speel EJM. Rapid Synthesis of Biotin-, Digoxigenin-, Trinitrophenyl-, and Fluorochrome-labeled Tyramides and Their Application for In Situ Hybridization Using CARD Amplification. J Histochem Cytochem [Internet]. 1998 [cited 2019 Mar 19];46:771–7. Available from: http://www.ncbi.nlm.nih.gov/pubmed/9603790 [PubMed: 9603790]
29. Uberoi A, Yoshida S, Lambert P. MmuPV1 L1- cytokeratin dual immunofluorescence using home-based tyramide signal amplification [Internet]. Protocols.io. 2017 [cited 2019 Mar 28]. Available from: https://www.protocols.io/view/untitled-protocol-i8cchsw
30. Martin D, Abba MC, Molinolo AA, Vitale-Cross L, Wang Z, Zaida M, et al. The head and neck cancer cell oncogenome: A platform for the development of precision molecular therapies. Oncotarget [Internet]. 2014 [cited 2019 Aug 6];5:8906–23. Available from: http://www.ncbi.nlm.nih.gov/pubmed/25275298 [PubMed: 25275298]
31. Swick AD, Prabakaran PJ, Miller MC, Javaid AM, Fisher MM, Sampene E, et al. Cotargeting mTORC and EGFR Signaling as a Therapeutic Strategy in HNSCC. Mol Cancer Ther [Internet]. 2017 [cited 2019 Aug 6];16:1257–68. Available from: http://www.ncbi.nlm.nih.gov/pubmed/28446642 [PubMed: 28446642]
32. Roy M, Li Z, Sacks DB. IQGAP1 Is a Scaffold for Mitogen-Activated Protein Kinase Signaling. Mol Cell Biol [Internet]. 2005 [cited 2019 Mar 6];25:7940–52. Available from: http://www.ncbi.nlm.nih.gov/pubmed/16135787 [PubMed: 16135787]

33. Wang X-X, Wang K, Li X-Z, Zhai L-Q, Qu C-X, Zhao Y, et al. Targeted knockdown of IQGAP1 inhibits the progression of esophageal squamous cell carcinoma in vitro and in vivo. Andl CD, editor. PLoS One [Internet]. 2014 [cited 2019 Mar 6];9:e96501 Available from: https://dx.plos.org/10.1371/journal.pone.0096501 [PubMed: 24800852]
34. Lu B, Lian R, Wu Z, Miao W, Li X, Li J, et al. MTA1 promotes viability and motility in nasopharyngeal carcinoma by modulating IQGAP1 expression. J Cell Biochem [Internet]. 2018 [cited 2019 Mar 6];119:3864–72. Available from: http://doi.wiley.com/10.1002/jcb.26494 [PubMed: 29125886]
35. Zhang T-T, Jiang Y-Y, Shang L, Shi Z-Z, Liang J-W, Wang Z, et al. Overexpression of DNAJB6 promotes colorectal cancer cell invasion through an IQGAP1/ERK-dependent signaling pathway. Mol Carcinog [Internet]. John Wiley & Sons, Ltd; 2015 [cited 2019 Mar 19];54:1205–13. Available from: http://doi.wiley.com/10.1002/mc.22194 [PubMed: 25044025]
36. Jin X, Pan Y, Wang L, Ma T, Zhang L, Tang AH, et al. Fructose-1,6-bisphosphatase Inhibits ERK Activation and Bypasses Gemcitabine Resistance in Pancreatic Cancer by Blocking IQGAP1–MAPK Interaction. Cancer Res [Internet]. American Association for Cancer Research; 2017 [cited 2019 Mar 19];77:4328–41. Available from: http://www.ncbi.nlm.nih.gov/pubmed/28720574 [PubMed: 28720574]
37. Wang S, Watanabe T, Noritake J, Fukata M, Yoshimura T, Itoh N, et al. IQGAP3, a novel effector of Rac1 and Cdc42, regulates neurite outgrowth. J Cell Sci [Internet]. 2007 [cited 2019 Mar 11];120:567–77. Available from: http://jcs.biologists.org/cgi/doi/10.1242/jcs.03356 [PubMed: 17244649]
38. Monteleon CL, McNeal A, Duperret EK, Oh SJ, Schapira E, Ridky TW. IQGAP1 and IQGAP3 Serve Individually Essential Roles in Normal Epidermal Homeostasis and Tumor Progression. J Invest Dermatol [Internet]. 2015 [cited 2019 Mar 11];135:2258–65. Available from: https://linkinghub.elsevier.com/retrieve/pii/S0022202X15389946 [PubMed: 25848980]
39. Nojima H, Adachi M, Matsui T, Okawa K, Tsukita S, Tsukita S. IQGAP3 regulates cell proliferation through the Ras/ERK signalling cascade. Nat Cell Biol [Internet]. 2008 [cited 2019 Mar 11];10:971–8. Available from: http://www.nature.com/articles/ncb1757 [PubMed: 18604197]
40. Yang Y, Zhao W, Xu Q-W, Wang X-S, Zhang Y, Zhang J. IQGAP3 promotes EGFR-ERK signaling and the growth and metastasis of lung cancer cells. Kalinichenko VV., editor. PLoS One [Internet]. 2014 [cited 2019 Mar 11];9:e97578 Available from: https://dx.plos.org/10.1371/journal.pone.0097578 [PubMed: 24849319]
41. Zoheir KM, Abd-Rabou AA, Harisa GI, Kumar A, Ahmad SF, Ansari MA, et al. IQGAP1 gene silencing induces apoptosis and decreases the invasive capacity of human hepatocellular carcinoma cells. Tumour Biol [Internet]. 2016 [cited 2019 Mar 11];37:13927–39. Available from: http://link.springer.com/10.1007/s13277-016-5283-8 [PubMed: 27488117]
42. Jin X, Liu Y, Liu J, Lu W, Liang Z, Zhang D, et al. The Overexpression of IQGAP1 and β-Catenin Is Associated with Tumor Progression in Hepatocellular Carcinoma In Vitro and In Vivo. Samant R, editor. PLoS One [Internet]. 2015 [cited 2019 Mar 11];10:e0133770 Available from: https://dx.plos.org/10.1371/journal.pone.0133770 [PubMed: 26252773]
43. Su D, Liu Y, Song T. Knockdown of IQGAP1 inhibits proliferation and epithelial-mesenchymal transition by Wnt/β-catenin pathway in thyroid cancer. Onco Targets Ther [Internet]. 2017 [cited 2019 Mar 11];10:1549–59. Available from: https://www.dovepress.com/knockdown-of-iqgap1-inhibits-proliferation-and-epithelial-mesenchymal-peer-reviewed-article-OTT [PubMed: 28352188]
44. Carmon KS, Gong X, Yi J, Thomas A, Liu Q. RSPO-LGR4 functions via IQGAP1 to potentiate Wnt signaling. Proc Natl Acad Sci U S A [Internet]. 2014 [cited 2019 Mar 11];111:E1221–9. Available from: http://www.pnas.org/lookup/doi/10.1073/pnas.1323106111 [PubMed: 24639526]
45. Nyman PE, Buehler D, Lambert PF. Loss of Function of Canonical Notch Signaling Drives Head and Neck Carcinogenesis. Clin Cancer Res [Internet]. 2018 [cited 2019 Mar 28];24:6308–18. Available from: http://www.ncbi.nlm.nih.gov/pubmed/30087145 [PubMed: 30087145]
46. Gorman JA, Babich A, Dick CJ, Schoon RA, Koenig A, Gomez TS, et al. The cytoskeletal adaptor protein IQGAP1 regulates TCR-mediated signaling and filamentous actin dynamics. J Immunol [Internet]. NIH Public Access; 2012 [cited 2019 Aug 8];188:6135–44. Available from: http://www.ncbi.nlm.nih.gov/pubmed/22573807 [PubMed: 22573807]

47. Sharma S, Findlay GM, Bandukwala HS, Oberdoerffer S, Baust B, Li Z, et al. Dephosphorylation of the nuclear factor of activated T cells (NFAT) transcription factor is regulated by an RNA-protein scaffold complex. Proc Natl Acad Sci [Internet]. 2011 [cited 2019 Aug 8];108:11381–6. Available from: http://www.ncbi.nlm.nih.gov/pubmed/21709260 [PubMed: 21709260]

48. Kanwar N, Wilkins JA. IQGAP1 involvement in MTOC and granule polarization in NK-cell cytotoxicity. Eur J Immunol [Internet]. 2011 [cited 2019 Aug 8];41:2763–73. Available from: http://www.ncbi.nlm.nih.gov/pubmed/21681737 [PubMed: 21681737]

49. Abel AM, Tiwari AA, Gerbec ZJ, Siebert JR, Yang C, Schloemer NJ, et al. IQ Domain-Containing GTPase-Activating Protein 1 Regulates Cytoskeletal Reorganization and Facilitates NKG2D-Mediated Mechanistic Target of Rapamycin Complex 1 Activation and Cytokine Gene Translation in Natural Killer Cells. Front Immunol [Internet]. Frontiers Media SA; 2018 [cited 2019 Aug 8]; 9:1168 Available from: http://www.ncbi.nlm.nih.gov/pubmed/29892299 [PubMed: 29892299]

50. Okada M, Hozumi Y, Iwazaki K, Misaki K, Yanagida M, Araki Y, et al. DGKζ is involved in LPS-activated phagocytosis through IQGAP1/Rac1 pathway. Biochem Biophys Res Commun [Internet]. 2012 [cited 2019 Aug 8];420:479–84. Available from: http://www.ncbi.nlm.nih.gov/pubmed/22450320 [PubMed: 22450320]

51. Brandt DT, Marion S, Griffiths G, Watanabe T, Kaibuchi K, Grosse R. Dia1 and IQGAP1 interact in cell migration and phagocytic cup formation. J Cell Biol [Internet]. 2007 [cited 2019 Aug 8]; 178:193–200. Available from: http://www.ncbi.nlm.nih.gov/pubmed/17620407 [PubMed: 17620407]

52. Chung LK, Philip NH, Schmidt VA, Koller A, Strowig T, Flavell RA, et al. IQGAP1 is important for activation of caspase-1 in macrophages and is targeted by Yersinia pestis type III effector YopM. MBio [Internet]. American Society for Microbiology (ASM); 2014 [cited 2019 Aug 8]; 5:e01402–14. Available from: http://www.ncbi.nlm.nih.gov/pubmed/24987096 [PubMed: 24987096]

TRANSLATIONAL RELEVANCE

Head and neck cancer (HNC) is the sixth most common cancer with a 5-year survival rate less than 50%. A frequently altered pathways in HNC is EGFR and its downstream PI3K signaling, which can be scaffolded by IQGAP1. Herein, we investigated the role of IQGAP1 in HNC using a combination of *in vitro* and *in vivo* approaches in human and mouse tissues/cell lines. We demonstrate that IQGAP1 is necessary for efficient PI3K signaling *in vitro* and *in vivo*, and the loss of IQGAP1 significantly reduced cancer phenotypes in mice. PI3K signaling was reduced in HNC arising in *Igqap1-knockout* mice, supporting that IQGAP1 contributes to HNC, at least partly through scaffolding PI3K. High IQGAP1 levels correlated with high pS6 levels in HNC patients. Importantly, high IQGAP1 levels correlated with poor survival in HNC patients, implicating its importance. Drugs that target IQGAP1 may provide new approaches treat HNC patients.

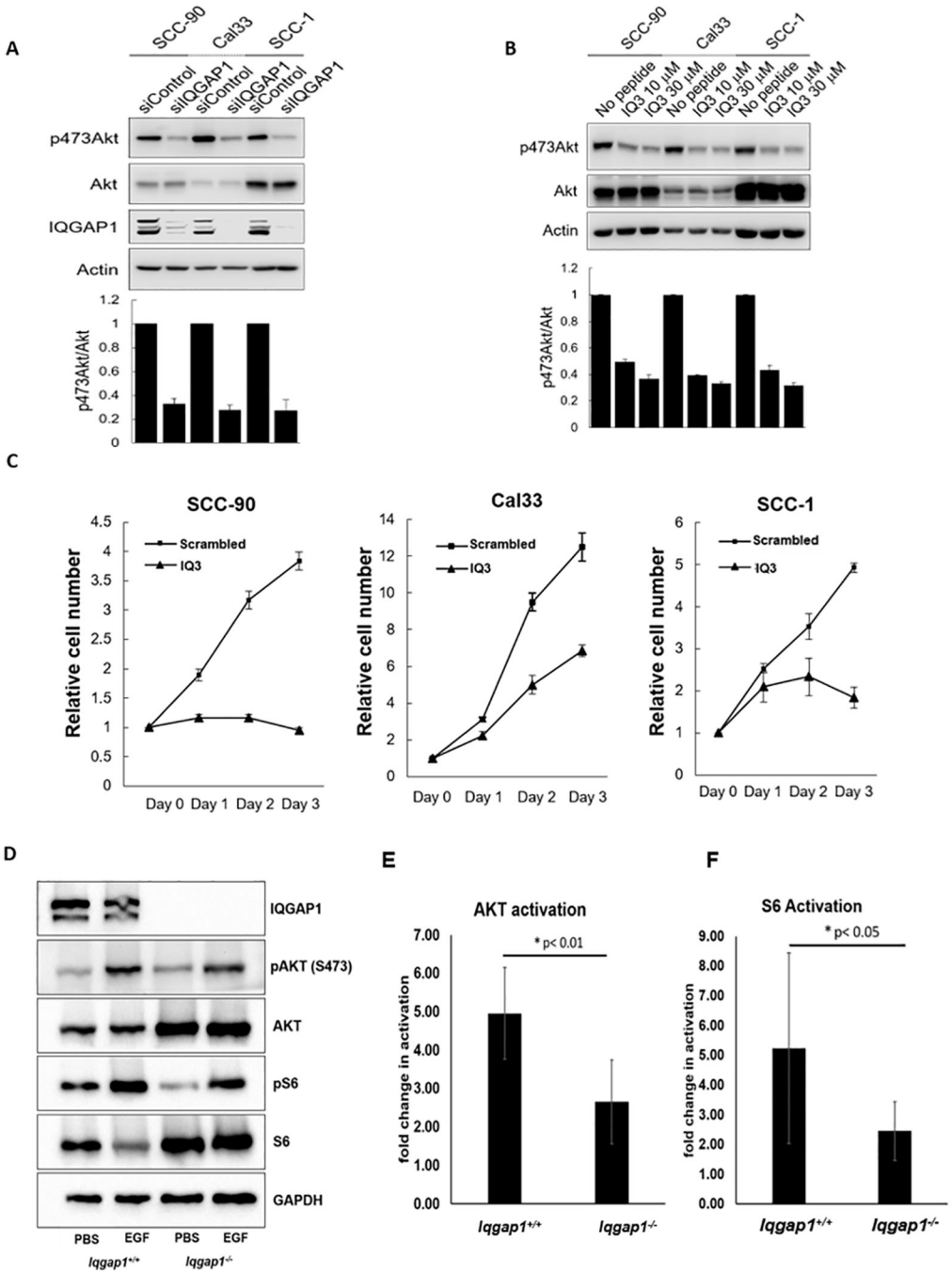

Figure 1. IQGAP1 is necessary for efficient PI3K signaling both *in vitro* and *in vivo*.

A) Requirement for IQGAP1 *in vitro*. siControl or siIQGAP1 treated HNC cells were harvested and cell lysates were analyzed by immunoblotting with the indicated antibodies. Intensity of Immunoblots were quantified with *ImageJ* and the graphs were shown mean ± standard deviation of n=3 of independent experiments. B) IQGAP1 mediates PI3K signaling in HNC cells. HNC cells were treated with the cell permeable peptide IQ3, which interrupts the IQGAP1-PI3K signaling complex, for 72hr with daily media change, then lysed and analyzed by immunoblotting with indicated antibodies. C) IQGAP1-mediated PI3K

signaling is required for HNC cell line survival. HNC cells were treated with IQ3 peptides at 30 μM concentration for the indicated time. The number of viable cells was counted. The experiments were independently repeated 3 times and the graphs were shown mean ± standard deviation. D-F) IQGAP1 is necessary for efficient PI3K signaling upon EGF-stimulation *in vivo*. D) Immunoblots detecting pAKT(S473) and total AKT, p-S6 and total S6 and GAPDH (loading control) in harvested dorsal skin lysates. 5-week-old *Iqgap1*$^{+/+}$ and *Iqgap1*$^{-/-}$ mice were stimulated with subcutaneous injection of EGF (5 μg/g weight). PBS was injected in vehicle control groups. The volume of each band was measured and the phosphorylation levels of AKT and S6 were determined by taking ratios of the (phosphorylated-protein/ total protein) upon EGF stimulation compared to PBS control. The quantified activation levels of (E) AKT and (F) S6 and are shown. Error bars were calculated by calculating the standard deviation of the average of 5 or 6 replicates. T-test was used for statistical analysis.

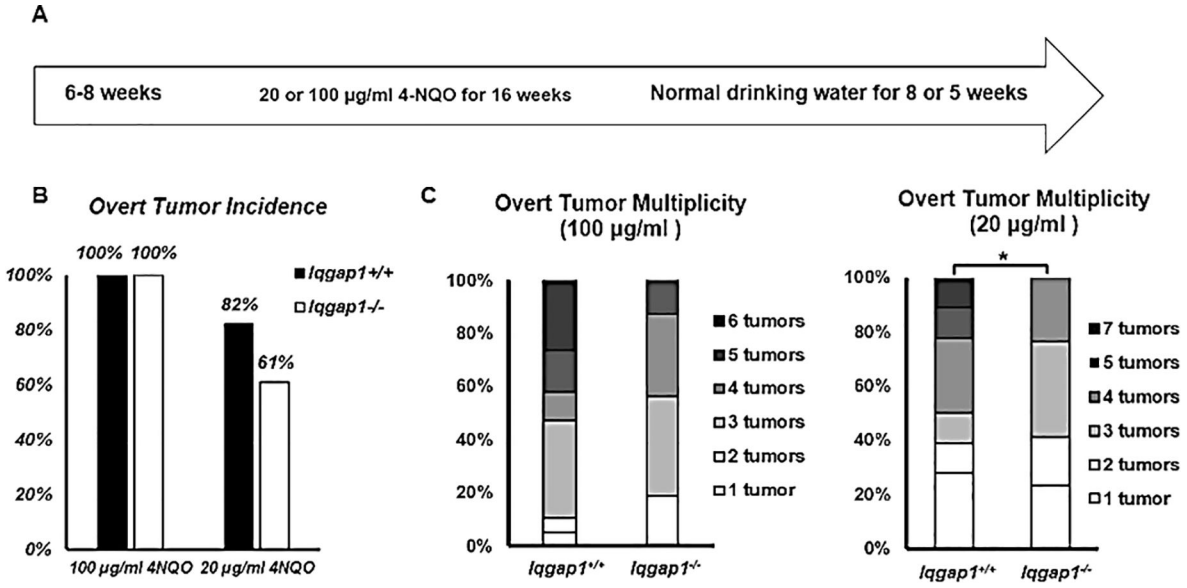

Figure 2. IQGAP1 contributes to head and neck tumorigenesis *in vivo*.

A) Treatment regimen of 4NQO, a synthetic oral carcinogen. Two dosages of 4NQO were given to mice. In 100 μg/ml treatment, groups of *Iqgap1*$^{+/+}$ (n=19) and *Iqgap1*$^{-/-}$ (n=16) mice were given 100 μg/ml 4NQO in their drinking water for 16 weeks, followed by 5 weeks of normal drinking water. In 20 μg/ml treatment, groups of *Iqgap1*$^{+/+}$ (n=22) and *Iqgap1*$^{-/-}$ (n=28) mice were given 20 μg/ml 4NQO in their drinking water for 16 weeks, followed by 8 weeks of normal drinking water. B) Overt tumor incidence. With 20 μg/ml 4NQO treatment, over tumor incidence in *Iqgap1*$^{+/+}$ mice vs. *Iqgap1*$^{-/-}$ mice not statistically significant (p=0.13, Fisher's exact test, two-sided). C) Overt tumor multiplicity. With 100 μg/ml 4NQO treatment, *Iqgap1*$^{+/+}$ *vs. Iqgap1*$^{-/-}$, mean: 3.95 vs. 3.37, p=0.29, Wilcoxon rank sum test, two-sided; with 20 μg/ml 4NQO treatment, *Iqgap1*$^{+/+}$ *vs. Iqgap1*$^{-/-}$, mean: 2.68 vs. 1.57, p=0.05, Wilcoxon rank sum test, two-sided.

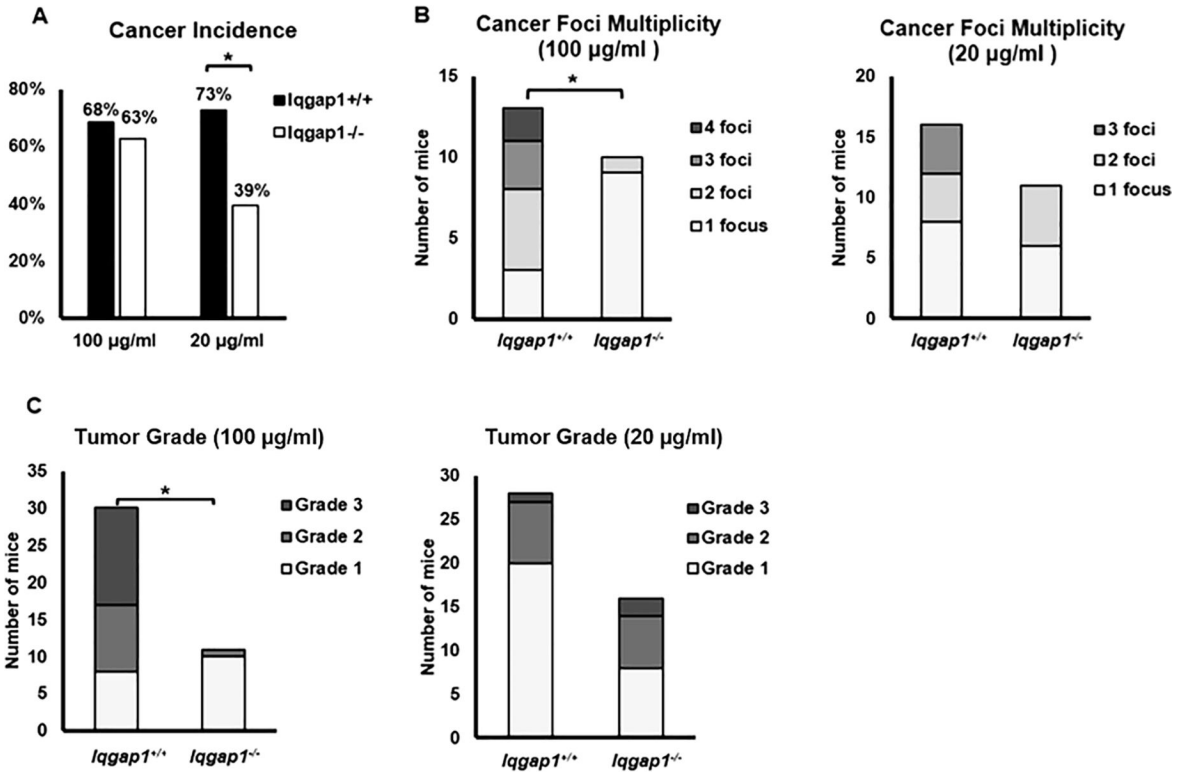

Figure 3. IQGAP1 contributes to head and neck carcinogenesis.

A) Incidence of invasive carcinoma. With 100 μg/ml 4NQO treatment, invasive carcinoma incidences between *Iqgap1*$^{+/+}$ vs. *Iqgap1*$^{-/-}$ mice were not significant (p=0.73, Fisher's exact test, two-sided). With 20 μg/ml 4NQO treatment, invasive carcinoma incidence was significantly lower in *Iqgap1*$^{-/-}$ mice than in *Iqgap1*$^{+/+}$ mice (p=0.02, Fisher's exact test, two-sided). B) Numbers of invasive carcinoma foci per mouse. With 100 μg/ml 4NQO treatment, *Iqgap1*$^{+/+}$ *vs. Iqgap1*$^{-/-}$: mean 2.3 vs. 1.1 foci per mouse, p<0.001, Wilcoxon rank sum test, two-sided; with 20 μg/ml 4NQO treatment, *Iqgap1*$^{+/+}$ *vs. Iqgap1*$^{-/-}$: mean: 1.75 vs. 1.45, p=0.46, Wilcoxon rank sum test, two-sided. C) Tumor grade for the invasive carcinomas. *Iqgap1*$^{+/+}$ *vs. Iqgap1*$^{-/-}$: mean: 5.1 vs. 4.1, p<0.001, Wilcoxon rank sum test, two-sided. With 20 μg/ml 4NQO treatment, *Iqgap1*$^{+/+}$ *vs. Iqgap1*$^{-/-}$: mean: 4.3 vs. 4.6, p=0.14, Wilcoxon rank sum test, two-sided.

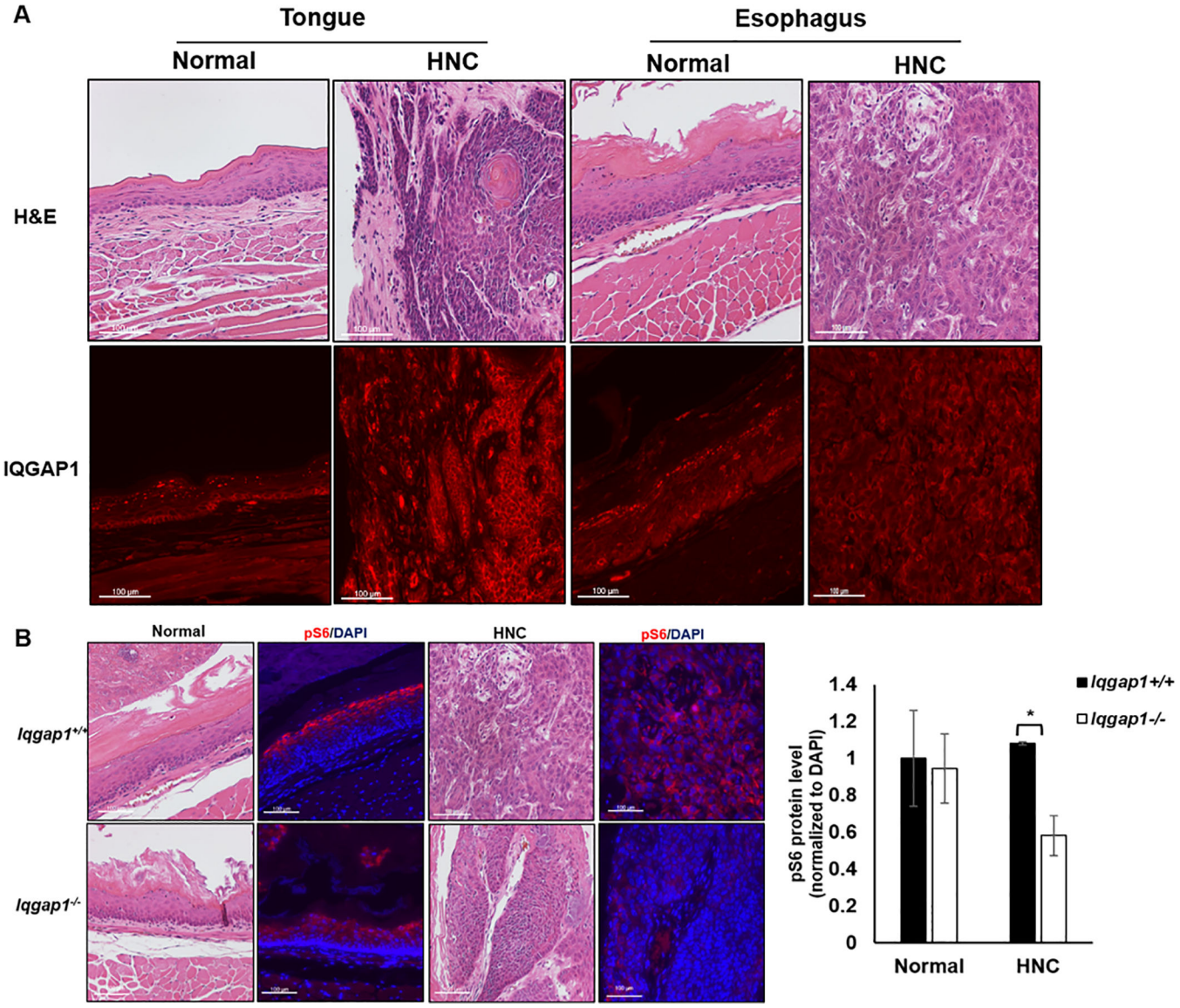

Figure 4. Biomarker analysis in 4NQO-treated mice.

A) IQGAP1 protein levels in normal and cancer regions (shown in H&E images) in both tongue and esophagus tissue of *Iqgap1*$^{+/+}$ mice (red, located mostly on cell membrane; levels of protein indicated by intensity of the signal). B) Immunofluorescence detecting pS6 in 4NQO-treated esophagus (normal, cancer, shown in the H&E images). Red: pS6, blue: DAPI. (left) Quantification of pS6 levels in normal and cancer tissues (right). Asterisk indicates statistically significance ($p<0.05$, T test, two-sided).

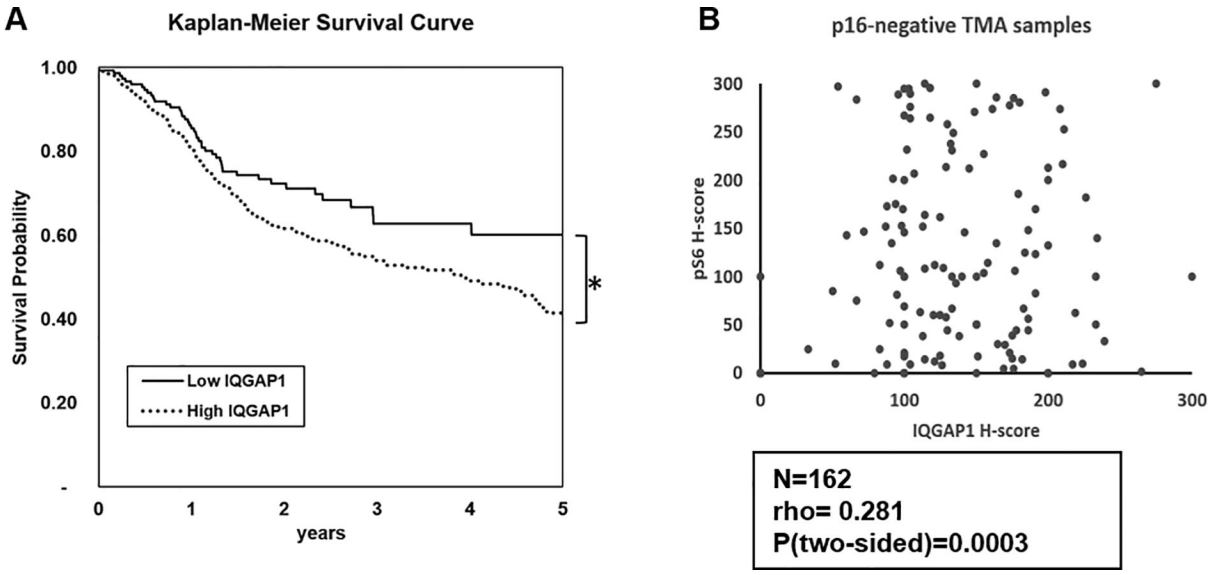

Figure 5. Analyzing the role of IQGAP1 in head and neck cancer patients.

A) High levels of IQGAP1 correlates with poorer survival in HNC patients. Kaplan-Meier curve was used to analyze how IQGAP1 expression level correlates with head and neck cancer survival, based on TCGA RNA database. Patients with higher IQGAP1 expression (N=346) results in poorer survival probability than those with lower IQGAP1 expression (N=153). The log-rank pValue< 0.0001, two-sided. B) Head and neck cancer TMA showed significant positive correlation between IQGAP1 and PI3K signaling, represented by pS6 level. Spearman Rank correlation test was performed in the p16-negative subset of samples (N=162), resulting in a coefficient rho=0.281, indicating a weak positive correlation the two markers. The observed positive correlation is statistically significant (p=0.0003, two-sided). The TMA slide was scanned and imaged by Vectra imaging system. Images were analyzed and quantified by inForm® Tissue Finder software. Levels of expression were reported as H-Scores

TABLE 1.

Disease severity in *Iqgap1+/+* and *Iqgap1*$^{-/-}$ mice treated with 100 μg/ml (Part A) or 20 μg/ml (Part B) 4NQO.

A. 100 μg/mL 4NQO for 16weeks +5 weeks of normal drinking water								
Total	n	Normal	Dysplasia			Carcinoma		
			Mild	Moderate	Severe	Well-differentiated (Grade1)	Moderate-differentiated (Grade2)	Poor-differentiated (Grade3)
Iqgap 1$^{+/+}$	19	0	1	1	4	2	5	6
Iqgap1$^{-/-}$	16	0	1	1	5	8	1	0
B. 20 μg/mL 4NQO for 16weeks +8 weeks of normal drinking water								
Total	n	Normal	Dysplasia			Carcinoma		
			Mild	Moderate	Severe	Well-differentiated (Grade1)	Moderate-differentiated (Grade2)	Poor-differentiated (Grade3)
Iqgap1$^{+/+}$	22	0	1	2	3	9	6	1
Iqgap1$^{-/-}$	28	0	5	2	10	4	5	2

Table Footnote: To determine whether there is a statistical difference in disease severity between *Iqgap1+/+* and *Iqgap1*$^{-/-}$ mice, each stage of disease, was assigned an integer from 0 to 6, the value increasing as the disease stage worsened, with normal (within normal limits) assigned a value of 0 and grade 3 carcinoma assigned a value of 6. Statistical analysis: Part A) Disease severity between *Iqgap1+/+* and *Iqgap1*$^{-/-}$ mice. Mean 4.42 vs. 3.43. p=0.01, Wilcoxon rank sum test, one-sided. Part B) Disease severity between *Iqgap1+/+* and *Iqgap1*$^{-/-}$ mice: Mean 3.91 vs. 3.28. p=0.05, Wilcoxon rank sum test, one-sided.